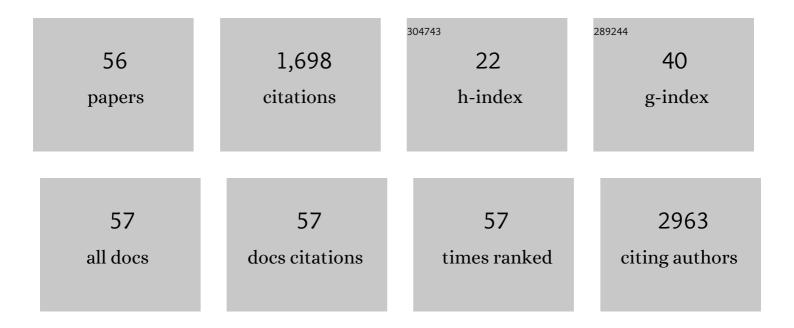
## Shawn Bourdo

List of Publications by Year in descending order

Source: https://exaly.com/author-pdf/6846438/publications.pdf Version: 2024-02-01



SHAWN ROLLEDO

#	Article	IF	CITATIONS
1	Phosphorous and nitrogen dual heteroatom doped mesoporous carbon synthesized via microwave method for supercapacitor application. Journal of Power Sources, 2014, 250, 257-265.	7.8	216
2	Organic Solar Cells: A Review of Materials, Limitations, and Possibilities for Improvement. Particulate Science and Technology, 2013, 31, 427-442.	2.1	150
3	Graphene supports <i>in vitro</i> proliferation and osteogenic differentiation of goat adult mesenchymal stem cells: potential for bone tissue engineering. Journal of Applied Toxicology, 2015, 35, 367-374.	2.8	122
4	Electrical, Optical, and Morphological Properties of P3HT-MWNT Nanocomposites Prepared by in Situ Polymerization. Journal of Physical Chemistry C, 2009, 113, 8023-8029.	3.1	97
5	Exceptional Superhydrophobicity and Low Velocity Impact Icephobicity of Acetone-Functionalized Carbon Nanotube Films. Langmuir, 2011, 27, 9936-9943.	3.5	96
6	Graphite/Polyaniline (GP) composites: Synthesis and characterization. Carbon, 2005, 43, 2983-2988.	10.3	71
7	Structural, Electrical, and Thermal Behavior of Graphiteâ€Polyaniline Composites with Increased Crystallinity. Advanced Functional Materials, 2008, 18, 432-440.	14.9	68
8	Oxygen Reduction Reaction Studies of Phosphorus and Nitrogen Coâ€Doped Mesoporous Carbon Synthesized via Microwave Technique. ChemElectroChem, 2014, 1, 573-579.	3.4	67
9	Graphene nanoparticles as osteoinductive and osteoconductive platform for stem cell and bone regeneration. Nanomedicine: Nanotechnology, Biology, and Medicine, 2017, 13, 2117-2126.	3.3	52
10	Tuning the work function of polyaniline via camphorsulfonic acid: an X-ray photoelectron spectroscopy investigation. RSC Advances, 2015, 5, 33-40.	3.6	49
11	Comparative Aging Study of Organic Solar Cells Utilizing Polyaniline and PEDOT:PSS as Hole Transport Layers. ACS Applied Materials & amp; Interfaces, 2015, 7, 27667-27675.	8.0	45
12	Ammonia Gas Sensing Behavior of Tanninsulfonic Acid Doped Polyaniline-TiO2 Composite. Sensors, 2015, 15, 26415-26429.	3.8	43
13	The role of surface chemistry in the cytotoxicity profile of graphene. Journal of Applied Toxicology, 2017, 37, 462-470.	2.8	38
14	Electrocatalytic and supercapacitor performance of Phosphorous and Nitrogen co-doped Porous Carbons synthesized from Aminated Tannins. Electrochimica Acta, 2015, 182, 987-994.	5.2	33
15	Optimization of the Protonation Level of Polyanilineâ€Based Holeâ€Transport Layers in Bulkâ€Heterojunction Organic Solar Cells. Energy Technology, 2013, 1, 463-470.	3.8	32
16	<p>Functionalized Graphene Nanoparticles Induce Human Mesenchymal Stem Cells to Express Distinct Extracellular Matrix Proteins Mediating Osteogenesis</p> . International Journal of Nanomedicine, 2020, Volume 15, 2501-2513.	6.7	27
17	Single-walled carbon nanotubes as specific targeting and Raman spectroscopic agents for detection and discrimination of single human breast cancer cells. Journal of Biomedical Optics, 2013, 18, 055003.	2.6	26
18	Hybrid Perovskite Photovoltaic Devices: Properties, Architecture, and Fabrication Methods. Energy Technology, 2017, 5, 373-401.	3.8	26

Shawn Bourdo

#	Article	IF	CITATIONS
19	Photovoltaic Device Performance of Single-Walled Carbon Nanotube and Polyaniline Films on n-Si: Device Structure Analysis. ACS Applied Materials & Interfaces, 2012, 4, 363-368.	8.0	25
20	Electrical and thermal properties of graphite/polyaniline composites. Journal of Solid State Chemistry, 2012, 196, 309-313.	2.9	25
21	Microwave-Assisted Synthesis of Nitrogen and Phosphorus Co-Doped Mesoporous Carbon and Their Potential Application in Alkaline Fuel Cells. Science of Advanced Materials, 2013, 5, 1275-1281.	0.7	25
22	Catalytic Conversion of Graphene into Carbon Nanotubes <i>via</i> Gold Nanoclusters at Low Temperatures. ACS Nano, 2012, 6, 501-511.	14.6	24
23	Optimizing Lignosulfonic Acid-Grafted Polyaniline as a Hole-Transport Layer for Inverted CH <sub>3</sub> NH <sub>3</sub> Pbl <sub>3</sub> Perovskite Solar Cells. ACS Omega, 2020, 5, 1887-1901.	3.5	23
24	Physicochemical characteristics of pristine and functionalized graphene. Journal of Applied Toxicology, 2017, 37, 1288-1296.	2.8	22
25	Functionalized gold nanorod nanocomposite system to modulate differentiation of human mesenchymal stem cells into neural-like progenitors. Scientific Reports, 2017, 7, 16654.	3.3	20
26	Polyurethane/nano-hydroxyapatite composite films as osteogenic platforms. Journal of Biomaterials Science, Polymer Edition, 2018, 29, 1426-1443.	3.5	18
27	Hierarchical ZnO Structure with Superhydrophobicity and High Adhesion. ChemPhysChem, 2011, 12, 2412-2414.	2.1	15
28	Graphene-based 2D constructs for enhanced fibroblast support. PLoS ONE, 2020, 15, e0232670.	2.5	14
29	Synthesis and characterization of tanninsulfonic acid doped polyaniline–metal oxide nanocomposites. Journal of Applied Polymer Science, 2012, 124, 3320-3328.	2.6	13
30	Phosphate removal from wastewater using novel renewable resource-based, cerium/manganese oxide-based nanocomposites. Environmental Science and Pollution Research, 2020, 27, 36688-36703.	5.3	13
31	Surface Passivation of Triple-Cation Perovskite via Organic Halide-Saturated Antisolvent for Inverted Planar Solar Cells. ACS Applied Energy Materials, 2021, 4, 3297-3309.	5.1	13
32	Evaluation of a Renewable Resource-based Carbon-Iron Oxide Nanocomposite for Removal of Arsenic from Contaminated Water. Journal of Macromolecular Science - Pure and Applied Chemistry, 2011, 48, 348-354.	2.2	12
33	T lymphocytes dominate local leukocyte infiltration in response to intradermal injection of functionalized grapheneâ€based nanomaterial. Journal of Applied Toxicology, 2017, 37, 1317-1324.	2.8	12
34	<i>p53</i> â€competent cells and <i>p53</i> â€deficient cells display different susceptibility to oxygen functionalized graphene cytotoxicity and genotoxicity. Journal of Applied Toxicology, 2017, 37, 1333-1345.	2.8	12
35	Evaluation of a bone filler scaffold for local antibiotic delivery to prevent Staphylococcus aureus infection in a contaminated bone defect. Scientific Reports, 2021, 11, 10254.	3.3	12
36	In vivo noninvasive analysis of graphene nanomaterial pharmacokinetics using photoacoustic flow cytometry. Journal of Applied Toxicology, 2017, 37, 1297-1304.	2.8	11

Shawn Bourdo

#	Article	IF	CITATIONS
37	Evaluation of a Polyurethane Platform for Delivery of Nanohydroxyapatite and Decellularized Bone Particles in a Porous Three-Dimensional Scaffold. ACS Applied Bio Materials, 2019, 2, 1815-1829.	4.6	11
38	Acid-free polyaniline:graphene-oxide hole transport layer in organic solar cells. Journal of Materials Science: Materials in Electronics, 2020, 31, 21640-21650.	2.2	11
39	Low-temperature (150°C) carbon nanotube growth on a catalytically active iron oxide–graphene nano-structural system. Journal of Catalysis, 2013, 299, 307-315.	6.2	10
40	Quantification of cellular associated graphene and induced surface receptor responses. Nanoscale, 2019, 11, 932-944.	5.6	10
41	Cytotoxicity profile of pristine graphene on brain microvascular endothelial cells. Journal of Applied Toxicology, 2019, 39, 966-973.	2.8	10
42	Catalytic effects of selected transition metal ions in the synthesis of lignosulfonic acid doped polyaniline. Journal of Applied Polymer Science, 2005, 98, 29-33.	2.6	9
43	Solar cells with graphene and carbon nanotubes on silicon. Journal of Experimental Nanoscience, 2013, 8, 565-572.	2.4	9
44	Genetic profiling of human bone marrow and adipose tissue-derived mesenchymal stem cells reveals differences in osteogenic signaling mediated by graphene. Journal of Nanobiotechnology, 2021, 19, 285.	9.1	9
45	Separation and spectroscopic/molecular weight analysis of crude and purified polyaniline(s). Journal of Polymer Research, 2013, 20, 1.	2.4	8
46	Calcium-channel blocking and nanoparticles-based drug delivery for treatment of drug-resistant human cancers. Therapeutic Delivery, 2014, 5, 763-780.	2.2	8
47	Novel Microwave-Assisted Synthesis of Nickel/Carbon (Ni/C) Nanocomposite with Tannin as the Carbon Source. Journal of Wood Chemistry and Technology, 2011, 31, 345-356.	1.7	7
48	Performance dependence of SWCNT/n-silicon hybrid solar cells on the charge carrier concentration in silicon substrates. RSC Advances, 2015, 5, 621-627.	3.6	7
49	Multiomics Evaluation of Human Fat-Derived Mesenchymal Stem Cells on an Osteobiologic Nanocomposite. BioResearch Open Access, 2020, 9, 37-50.	2.6	6
50	New Route of Microwave-Assisted Synthesis of Carbon-Supported Nickel Phosphide (C/Ni2P) Nanocomposite. Phosphorus, Sulfur and Silicon and the Related Elements, 2013, 188, 768-777.	1.6	3
51	Synthesis of "Naked―TeO <sub>2</sub> Nanoparticles for Biomedical Applications. ACS Omega, 2022, 7, 23685-23694.	3.5	3
52	Electrical transport properties of (110)-oriented PrBa2(Cu0.8Ga0.2)3O7 thin films. Applied Physics Letters, 2012, 100, 252601.	3.3	2
53	Novel Microwave-Assisted Synthesis of Renewable-Resource Based Carbon-Magnetite Nanocomposites. Journal of Wood Chemistry and Technology, 2012, 32, 268-278.	1.7	2
54	Dendritic cell biocompatibility of etherâ€based urethane films. Journal of Applied Toxicology, 2021, 41, 1456-1466.	2.8	2

#	Article	IF	CITATIONS
55	Improved efficiency of inverted planar perovskite solar cells with an ultrahigh work function doped polymer as an alternative hole transport layer. Journal of Materials Chemistry C, 2022, 10, 4411-4423.	5.5	2

Electrical transport and Raman spectral studies of (110)-oriented PrBa2 (Cu0.8M0.2)307 (M = Ga, Al, Zn,) Tj ETQq0.0 0 rgBT/Overlock 2